

# Finite Temperature Resonant Magnetotunneling in AlGaAs-GaAs-AlGaAs Heterostructures

Ø. Lund Bø,<sup>(1)</sup> Yu. Galperin,<sup>(1,2)</sup> and K. A. Chao,<sup>(3)</sup>

<sup>(1)</sup>*Department of Physics, University of Oslo, P. O. Box 1048 Blindern, N 0316 Oslo 3, Norway,*

<sup>(2)</sup> *A. F. Ioffe Physico-Technical Institute, 194021 St. Petersburg, Russia,*

<sup>(3)</sup>*Department of Physics, Norwegian Institute of Technology, The University of Trondheim,  
N 7034 Trondheim, Norway.*

(August 16, 2018)

## Abstract

We have analyzed the effect of electron-LO phonon interaction in a double-barrier resonant tunneling structure under a magnetic field  $\mathbf{B}$  applied parallel to the tunneling current. While the low temperature anti-crossing phenomenon has already been investigated, here we study the phonon absorption resonant magnetotunneling at finite temperatures. The Matsubara technique is used to sum up resonant diagrams of higher orders, and the result is selfconsistently renormalized. The phonon absorption tunneling spectrum has been calculated numerically. The result shows that the phonon-absorption process produces two broad inelastic wings on the main elastic tunneling peak, the strength of which is sensitive to the resonant condition, and grows with increasing temperature. The width of the inelastic wings are proportional to  $B^{1/2}$ . This is in contrast to the appearance of anti-crossing in the phonon emission tunneling process. The difference is due to the fact that the phonon emission is a coherent process, while the absorption is a typical incoherent

process since absorbed real phonons have random phases.

71.38.+i, 72.10.Di, 73.40.Kp

## I. INTRODUCTION

Since the pioneer work of Tsu and Esaki<sup>1</sup> and the observation of negative differential resistance by Sollner *et al.*<sup>2</sup>, there has been increasing interest in resonant tunneling through a double-barrier resonant tunneling structure (DBRTS) both experimentally and theoretically. Among the important tools of characterizing DBRTS, one is the DC transport<sup>3–7</sup> together with phonon induced or laser induced tunneling<sup>8–15</sup>. In connection to such characterization, the DC current noise of a DBRTS has also been investigated. A common feature of various resonant tunneling structures is the *inelastic* resonant tunneling due to the coupling of tunneling electrons to phonons. This phenomenon is not only interesting but also useful because it provides a way to investigate both electron modes and phonon modes. A theory of phonon assisted resonant tunneling through a DBRTS in the absence of an external magnetic field was presented by Wingreen *et al.*<sup>11</sup> and by Jonson<sup>14</sup>. Assuming a perfect sample without imperfection and impurity, in these works an exact solution was obtained when the system is reduced to one-dimension and when tunneling processes through different quasibound states in the well are decoupled. The problem becomes much complicated when these tunneling processes are coupled, for example by phonons.

Magnetic field is another important tool for sample characterization because of the formation of Landau level spectrum and the drastic modification of electronic wave functions, especially under strong external field. For a DBRTS, the challenging situation is when the magnetic **B** is applied parallel to the tunneling current **I**, as schematically illustrated in Fig. 1. To clarify the important features of Fig. 1, let us consider the experimentally most extensively studied DBRTS  $\text{GaAs}^+/\text{Al}_{0.3}\text{Ga}_{0.7}\text{As}/\text{GaAs}/\text{Al}_{0.3}\text{Ga}_{0.7}\text{As}/\text{GaAs}^+$ , with both the barrier width and the well width of the order of 40-60 Å. In this case the barrier height is about 300 meV, and in the well there exists only one quasibound state with energy  $\epsilon_b$ . We will set the zero reference energy at the bottom of the conduction band of the collector (labeled by *c*), and so the conduction band minimum of the emitter (labeled by *e*) is raised to *eV* by the bias *V*. Under a magnetic field **B** perpendicular to interfaces which are parallel

to the  $xy$ -plane, the quasibound energy level  $\epsilon_b$  splits into a series of discrete Landau levels  $\epsilon_b + (n + \frac{1}{2})\hbar\omega_c$ , where  $\omega_c = eB/m^*c$  is the cyclotron frequency in *GaAs*. The electronic energy levels in the emitter and collector, on the other hand, form sets of Landau bands  $eV + \epsilon_z(k_{e,z}) + (n_e + \frac{1}{2})\hbar\omega_c$  and  $\epsilon_z(k_{c,z}) + (n_c + \frac{1}{2})\hbar\omega_c$ , respectively, where  $\epsilon_z(k_z) = \hbar^2 k_z^2 / 2m^*$  is the kinetic energy along the tunneling direction.

Such level splitting has important influences on both elastic and phonon assisted tunneling<sup>16–18</sup>. In a perfect DBRTS, if the electron-phonon interaction is ignored the tunneling tunneling process conserves the Landau level quantum number ( $n_e = n = n_c$ ). If the magnetic field is sufficiently strong such that  $\hbar\omega_c$  is much larger than the thermal energy  $k_B T$ , the resonant tunneling is indeed one-dimensional with all tunneling channels decoupled from each other. The electron-phonon interaction mixes the channels. If the magnetic field is tuned into the resonant condition  $\hbar\omega_c = \hbar\omega_0$ , where  $\omega_0$  is the optical phonon frequency in *GaAs*, then the resonant tunneling processes through two adjacent Landau levels are resonantly coupled. In fact, this is one way to observe the strong renormalization of Landau levels due to the electron-phonon interaction<sup>19,20</sup>. In a 3D electron gas, the renormalization effect is proportional to  $g^{4/3}$ , while in a 2D system it is proportional to  $g$ , where  $g$  is the electron-phonon coupling constant to be defined later.

Under a strong magnetic field and at low temperatures, one relevant interesting phenomenon is the formation of magnetopolaron. Let us consider the simpler situation that only the lowest Landau band in the emitter ( $n_e = 0$ ) is occupied with quasi Fermi energy  $\epsilon_{e,F}$ . In a perfect DBRTS, one might expect to see in the  $I$ - $V$  characteristics the elastic resonant tunneling peak around the bias  $eV = \epsilon_b - \epsilon_{e,F}$ , with series of phonon replicas at  $eV = \epsilon_b + n\hbar\omega_c - \epsilon_{e,F} + \nu\hbar\omega_0$ , where  $\nu$  is an integer. However, complication arises when the condition  $\omega_c = (\nu - \nu')\omega_0/(n' - n)$  is satisfied. Then, an electron in the emitter can tunnel resonantly into two coherent degenerate states in the well: into the Landau level  $n$  by emitting  $\nu$  phonons, or into the Landau level  $n'$  by emitting  $\nu'$  phonons. The two final states are strongly hybridized because of the coherence, and so in phonon emission resonant magnetotunneling experiments, magnetopolarons have been observed<sup>20,21</sup>. A standard way

to present such experimental data is to plot resonant tunnelings peak position as a function of the magnetic field and the bias voltage. In this two-dimensional plot, the existence of magnetopolarons is reflected by the *anti-crossing*.

A phonon emission resonant magnetotunneling process leading to two coherent final states, indicated as  $E0$  and  $E1$ , is illustrated in part (a) of Fig. 2, where the thick lines form the Landau fan in the emitter, and the thin lines form the Landau fan in the well. Under this resonant condition, the  $I$ - $V$  characteristics will exhibit two resolved peaks of almost equal strength<sup>20,22</sup>. A similar diagram for phonon absorption resonant magnetotunneling is demonstrated in part (b) of Fig. 2. Here again we assume that only the lowest Landau level in the emitter is occupied, and the bias is tuned into elastic resonant tunneling  $eV = \varepsilon_b - \varepsilon_{e,F}$ . Then, the two sets of Landau fans coincide with each other. At the magnetic field strength  $\hbar\omega_c = \hbar\omega_0$ , an electron in the emitter having the proper energy can tunnel resonantly into the state  $A0$  elastically, or into the state  $A1$  by absorbing a phonon. We are interested in finding out how the energy levels  $A0$  and  $A1$  would be modified when they are resonantly coupled by phonons. In other words, we would like to derive the resulting transmission spectrum when the phonon absorption resonant magnetotunneling takes place.

The essential issue here is the coherence. Since absorbed thermal phonons have random phases, they can not participate in coherent process. This problem was investigated in our recent work<sup>22</sup>, where relevant references are listed. However, this work is based on a low order perturbation expansion, together with an exponential renormalization (see e. g. Ref. 23). In the vicinity of resonance, low order perturbation expansion is not sufficiently accurate. In the present work we improve our previous results with an infinite summation of resonant diagrams and a selfconsistent renormalization. Analytical expressions can be derived under the reasonable assumption of a dispersionless longitudinal optical (LO) phonon branch. To present a complete analysis, we will treat both the phonon emission and the phonon absorption resonant magnetotunneling.

Sec. II describes our model Hamiltonian, from which the transmission probability and the differential conductance will be derived in Sec. III. The self-energy and the vertex correction

will first be analyzed at low order for the general case, and then be summed up to all orders for a model two-level system, which contains the essential physics for phonon assisted resonant magnetotunneling through a DBRTS. This will be done in Sec. VI, and the so-obtained self-energy is renormalized selfconsistently in Sec. V. Numerical results will be presented in Sec. VI, followed by some remarks in the last Sec. VII. The electron-phonon scattering matrix elements are calculated in Appendix A.

## II. THE MODEL

To describe our model system, let us refer to Fig. 1 which specifies the potential and various energy levels of a DBRTS under a bias  $V$ , with zero reference energy set at the conduction band minimum of the collector. We assume the same material for the emitter, the well, and the collector, and also assume only one quasibound level  $\epsilon_b$  in the well, which is usually the case for realistic samples. In our model we will ignore the scattering due to the interface roughness and impurities. Since the magnetic field  $\mathbf{B}$  is applied in the positive direction of  $z$ -axis perpendicular to interfaces, it is convenient to choose the Landau gauge with the vector potential  $\mathbf{A}=(0, Bx, 0)$ .

The eigenstates in the well are labeled by the Landau level quantum number  $n$  and the index of degeneracy  $k_y$ . However, in the emitter (or collector), besides the similar quantum numbers  $(n_e, k_{e,y})$  [or  $(n_c, k_{c,y})$ ], we need also to specify the kinetic energy  $\epsilon_z(k_{e,z})$  [or  $\epsilon_z(k_{c,z})$ ] of an electron along the tunneling direction. For the convenience of presenting mathematical formulas, we define the simplified notation  $\alpha \equiv (n, k_y)$  for the states in the well, and  $\beta \equiv (n_j, k_{j,y}, k_{j,z})$ , where  $j=e$  for the emitter, and  $j=c$  for the collector. In terms of these notations, the normalized eigenstates and the eigenvalues are

$$\phi_\alpha(\mathbf{r}) = \chi(z) \exp(ik_y y) \varphi_n(x + l^2 k_y), \quad (1)$$

$$E_\alpha = \epsilon_b + \epsilon_n \equiv \epsilon_b + \hbar\omega_c(n + \frac{1}{2}) \quad (2)$$

in the well, and

$$\phi_{j,\beta}(\mathbf{r}) = \exp(ik_{j,z}z + ik_{j,y}y)\varphi_n(x + l^2k_{j,y}) , \quad (3)$$

$$\begin{aligned} E_{j,\beta} &= eV\delta_{j,e} + \epsilon_z(k_{j,z}) + \varepsilon_{n_j} \\ &\equiv eV\delta_{j,e} + \epsilon_z(k_{j,z}) + \hbar\omega_c(n_j + \frac{1}{2}) \end{aligned} \quad (4)$$

in the emitter ( $j = e$ ) under the bias  $eV$ , and the collector ( $j = c$ ). Here  $l = \sqrt{c\hbar/eB}$  is the magnetic length.

Using this set of basis functions, our model system in Fig. 1 can be described with the tunneling Hamiltonian

$$\mathcal{H} = \mathcal{H}_e + \mathcal{H}_{ph} + \mathcal{H}_{e-ph} . \quad (5)$$

The electronic part of the Hamiltonian with an external magnetic field is given by

$$\begin{aligned} \mathcal{H}_e &= \sum_{j,\beta} E_{j,\beta} c_{j,\beta}^\dagger c_{j,\beta} + \sum_{\alpha} E_{\alpha} c_{\alpha}^\dagger c_{\alpha} \\ &\quad + \sum_{j,\alpha,\beta} [V_{j,\beta\alpha} c_{\alpha}^\dagger c_{j,\beta} + h.c.] . \end{aligned} \quad (6)$$

The tunnel matrix elements  $V_{j,\beta\alpha}$  have to be calculated using the eigenstates listed above. Since the interfaces are assumed to be perfect, the momentum  $\mathbf{k}_{\parallel}$  parallel to interfaces remains invariant during the tunneling through a potential barrier. Both the Landau level index and  $k_y$  are then conserved, and so the calculation of the matrix elements  $V_{j,\beta\alpha}$  reduces to the solving of a one-dimensional Schrödinger equation<sup>24</sup>, following with the application of the Bardeen's prescription<sup>25</sup>.

Electrons interact with LO phonons. Here we will neglect the weak phonon dispersion, and the resulting phonon Hamiltonian is simply

$$\mathcal{H}_{ph} = \hbar\omega_0 \sum_{\mathbf{q}} b_{\mathbf{q}}^\dagger b_{\mathbf{q}} . \quad (7)$$

Since electrons in the well has a finite life time, it is reasonable to expect that the dominating contribution to electron-LO phonon interaction comes from the situation when electrons occupy the quasibound state in the well<sup>14</sup>. In terms of the Frölich Hamiltonian<sup>23</sup>, the electron-LO phonon interaction can be expressed as

$$\mathcal{H}_{\text{e-ph}} = \sum_{\alpha, \alpha_1, \mathbf{q}} M_{\alpha\alpha_1}(\mathbf{q}) (b_{\mathbf{q}}^\dagger + b_{\mathbf{q}}) c_{\alpha_1}^\dagger c_\alpha, \quad (8)$$

where  $\alpha = (n, k_y)$ ,  $\alpha_1 = (n_1, k_y - q_y)$ , and

$$\begin{aligned} M_{\alpha\alpha_1}(\mathbf{q}) &\equiv \frac{M}{\sqrt{V_0}q} \int \phi_{\alpha_1}^*(\mathbf{r}) e^{i\mathbf{q}\cdot\mathbf{r}} \phi_\alpha(\mathbf{r}) d\mathbf{r}, \\ M^2 &= \pi e^2 \hbar \omega_0 \left( \frac{1}{\epsilon_\infty} - \frac{1}{\epsilon_0} \right). \end{aligned} \quad (9)$$

The above Hamiltonian describes the general case. We are interested in the phonon absorption resonant magnetotunneling process as illustrated by part (b) in Fig. 2. Since the cross section for multiphonon absorption is much smaller than that for single phonon absorption, our problem can be well represented by retaining only the two lowest Landau levels  $n = 0$  and  $n = 1$ . With low impurity concentration in the emitter such that only the lowest Landau level  $n_e = 0$  in the emitter is occupied, the resulting two-level system can be solved exactly. This exact solution can be extended to study the phonon emission resonant magnetotunneling if the process demonstrated by part (a) in Fig. 2 will be modified as follows. We first increase the impurity concentration in the emitter such that under very strong magnetic field, only the two lowest Landau levels  $n_e = 0$  and  $n_e = 1$  are occupied. Next we set the bias at  $eV = \epsilon_b + \hbar\omega_0 - \epsilon_{e,F}$ . Then, when the magnetic field is tuned to  $\hbar\omega_c = \hbar\omega_0$ , electrons in the second Landau level ( $n_e = 1$ ) in the emitter can tunnel resonantly either into the  $E1$  state via an elastic process, and into the  $E0$  state by emitting a phonon. This is again a resonant tunneling in a two-level system with two coherent degenerate final states.

In the rest of this paper, we will first perform a general theoretical analysis. Then we will continue to study in details this exactly solvable two-level system.

### III. TRANSMISSION PROBABILITY

To calculate the conductance of a DBRTS, we must first calculate the transmission probability of an electron from the initial state  $(n_e, k_{e,y}, k_{e,z})$  in the emitter with energy  $\varepsilon$  to

the final state  $(n_c, k_{c,y}, k_{c,z})$  in the collector with energy  $\varepsilon_1$ . This transmission probability can be expressed in terms of the Fourier transform of the two-particle Green's function as<sup>11</sup>

$$T_{\alpha\alpha_1}(\varepsilon, \varepsilon_1) = \gamma_e(\varepsilon)\gamma_c(\varepsilon_1) \times \int \frac{d\tau ds dt}{2\pi\hbar^3} e^{i[(\varepsilon-\varepsilon_1)\tau+\varepsilon_1 t-\varepsilon s]/\hbar} K_{\alpha\alpha_1}(\tau, s, t), \quad (10)$$

where

$$K_{\alpha\alpha_1}(\tau, s, t) = \Theta(s)\Theta(t) \times \langle c_\alpha(\tau-s)c_{\alpha_1}^\dagger(\tau)c_{\alpha_1}(t)c_\alpha^\dagger(0) \rangle \quad (11)$$

is the so-called *transmission Green's function*. Here  $\alpha = (n, k_y) \equiv (n_e, k_{e,y})$  and  $\alpha_1 = (n_1, k_{1y}) \equiv (n_c, k_{c,y})$  label two electronic states in the well.  $\gamma_j(\varepsilon) = 2\pi \sum_\beta |V_{j,\beta\alpha}|^2 \delta(\varepsilon - E_{j,\beta})$  is the escape rate of an electron from the well to the emitter  $j = e$  or the collector  $j = c$ . The total escape rate from the well is simply  $\gamma(\varepsilon) = \gamma_e(\varepsilon) + \gamma_c(\varepsilon)$ .

It can be shown<sup>11,14,26</sup> that the Fourier transform  $K_{\alpha\alpha_1}(\varepsilon, \varepsilon_1)$  of  $K_{\alpha\alpha_1}(\tau, s, t)$  is in fact equivalent to a two-particle Green's function with input energies  $(\varepsilon, \varepsilon_1 - \Omega)$  and output energies  $(\varepsilon_1, \varepsilon - \Omega)$ , analytically continued into the upper half plane of the complex variables  $(\varepsilon, \varepsilon_1)$  and into the lower half plane of the complex variables  $(\varepsilon - \Omega, \varepsilon_1 - \Omega)$ . This two-particle Green's function is schematically illustrated in Fig. 3. The diagrammatic technique for an interacting electron-phonon system under a uniform external magnetic field has been extensively discussed in the literature<sup>27–29</sup>, and here we will follow the conventional approach. After completing such calculation and then setting  $\Omega \rightarrow 0$ , we obtain  $K_{\alpha\alpha_1}(\varepsilon, \varepsilon_1)$  and

$$T_{\alpha\alpha_1}(\varepsilon, \varepsilon_1) = \gamma_e(\varepsilon)\gamma_c(\varepsilon_1)K_{\alpha\alpha_1}(\varepsilon, \varepsilon_1). \quad (12)$$

If there is no electron-LO phonon scattering,  $K_{\alpha\alpha_1}(\varepsilon, \varepsilon_1)$  can be readily derived from the electronic Hamiltonian  $\mathcal{H}_e$  as

$$K_{\alpha\alpha_1}(\varepsilon, \varepsilon_1) = \frac{\delta(\varepsilon - \varepsilon_1)\delta_{\alpha\alpha_1}}{(\varepsilon - E_\alpha)^2 + (\gamma/2)^2}. \quad (13)$$

The total transparency is defined as

$$T_\alpha(\varepsilon) = \int \sum_{\alpha_1} T_{\alpha\alpha_1}(\varepsilon, \varepsilon_1) d\varepsilon_1, \quad (14)$$

with the corresponding correlation function

$$K_\alpha(\varepsilon) = \int \sum_{\alpha_1} K_{\alpha\alpha_1}(\varepsilon, \varepsilon_1) d\varepsilon_1. \quad (15)$$

In the wide band approximation, where the energy dependence of  $\gamma_e$  and  $\gamma_c$  can be neglected,  $T_\alpha(\varepsilon)$  and  $K_\alpha(\varepsilon)$  are simply connected as

$$T_\alpha(\varepsilon) = \gamma_e \gamma_c K_\alpha(\varepsilon). \quad (16)$$

Therefore, our task is to investigate the correlation function  $K_\alpha(\varepsilon)$ .

In terms of diagrams,  $K_\alpha(\varepsilon)$  is represented in Fig. 4. In this figure the arrowed double line towards right (or left) is the dressed one-electron retarded (or advanced) Green's function  $G_R(\alpha, \varepsilon)$  [or  $G_A(\alpha, \varepsilon - \Omega)|_{\Omega \rightarrow 0}$ ] of the entire system including the electron-phonon interaction, where the horizontal arrowed single lines are the corresponding bare one-electron Green's functions  $G_R^{(0)}(\alpha, \varepsilon)$  and  $G_A^{(0)}(\alpha, \varepsilon - \Omega)|_{\Omega \rightarrow 0}$  of the electronic system without the electron-phonon interaction. If an arrowed single line is tilted away from the horizontal direction, the variables in the corresponding Green's function should be summed up. All retarded (or advanced) Green's function are analytically continued into the upper (or lower) half plane of the complex variable  $\varepsilon$ . Based on this diagram,  $K_\alpha(\varepsilon)$  consists of two terms

$$K_\alpha(\varepsilon) = K_\alpha^0(\varepsilon) + K_\alpha^v(\varepsilon). \quad (17)$$

The first term is just a product of the two analytically continued dressed one-electron Green's functions

$$K_\alpha^0(\varepsilon) = |G_R(\alpha, \varepsilon)|^2. \quad (18)$$

The second term is the vertex part, which can be expressed as

$$K_\alpha^v(\varepsilon) = |G_R(\alpha, \varepsilon)|^2 \mathcal{K}(\alpha, \varepsilon). \quad (19)$$

Let us first consider the Green's function  $G_R(\alpha, \varepsilon)$ . To study the effect of electron-LO phonon interaction on the Green's function, we will use the Matsubara technique<sup>23,30</sup>. From the Dyson equation for the Matsubara Green's function

$$\begin{aligned}\mathcal{G}(\alpha, \varepsilon) &= \frac{\mathcal{G}^{(0)}(\alpha, \varepsilon)}{1 - \mathcal{G}^{(0)}(\alpha, \varepsilon)\Sigma(\alpha, \varepsilon)} \\ &= \frac{1}{\varepsilon - E_\alpha + \frac{i}{2}\delta - \Sigma(\alpha, \varepsilon)},\end{aligned}\quad (20)$$

where  $\delta \equiv \gamma \text{sign}(\text{Im}[\varepsilon])$ , and

$$\mathcal{G}^{(0)}(\alpha, \varepsilon) = \frac{1}{\varepsilon - E_\alpha + i\delta/2} \quad (21)$$

with discrete Fermion frequencies  $\varepsilon = i\pi(2n + 1)k_B T$ , it is clear that we need to calculate the self-energy  $\Sigma(\alpha, \varepsilon)$ . While the self-energy will be analyzed in details later to all orders of electron-phonon interaction, to the lowest order shown in Fig. 5a, we have

$$\begin{aligned}\Sigma(\alpha, \varepsilon) &= -k_B T \sum_{\varepsilon_1, \alpha_1, \mathbf{q}} \mathcal{G}^{(0)}(\alpha_1, \varepsilon_1) \mathcal{D}^{(0)}(\mathbf{q}, \varepsilon - \varepsilon_1) \\ &\quad \times |M_{\alpha\alpha_1}(\mathbf{q})|^2,\end{aligned}\quad (22)$$

where

$$\mathcal{D}^{(0)}(\mathbf{q}, \omega) = \frac{2\hbar\omega_0(q)}{\omega^2 - \hbar^2\omega_0^2(q)} \quad (23)$$

with discrete Boson frequencies  $\omega = i\pi 2n k_B T$ .

To the same order as the above self-energy, the vertex correction  $\mathcal{K}(\alpha, \varepsilon)$  in (19), with the corresponding diagram Fig. 5b, can be expressed as

$$\begin{aligned}\mathcal{K}(\alpha, \varepsilon) &= 2\pi k_B T \sum_{\alpha_1, \varepsilon_1, \vec{q}} |M_{\alpha\alpha_1}(\mathbf{q})|^2 \\ &\quad \times \mathcal{D}^{(0)}(\varepsilon - \varepsilon_1) \mathcal{G}^{(0)}(\alpha_1, \varepsilon_1) \mathcal{G}^{(0)}(\alpha_1, \varepsilon_1 - \Omega).\end{aligned}\quad (24)$$

The factor  $2\pi k_B T$  in front of this expression is due to the fact that the  $\varepsilon_1$  integration in (14) has been replaced by a summation over the discrete Matsubara energies. Comparing this expression to (22) for self-energy, we expect a relation between  $\mathcal{K}(\alpha, \varepsilon)$  and  $\Sigma(\alpha, \varepsilon)$ . This will be clarified in the next section.

Now we have set up the scheme to calculate the transmission probability with (16)-(19) and (24). Knowing the transmission probability, the tunneling current through a DBRTS can be calculated from<sup>11</sup>

$$J(V) = \frac{e}{\pi\hbar} \int \sum_{\alpha} T_{\alpha}(\varepsilon) \times [f_e(\varepsilon - eV) - f_c(\varepsilon)] d\varepsilon, \quad (25)$$

where

$$f_j(\varepsilon) = \left[ \exp \left( \frac{\varepsilon - \epsilon_{j,F}}{k_B T} \right) + 1 \right]^{-1}$$

is the Fermi distribution function in the emitter (or collector) for  $j = e$  (or  $j = c$ ) with the Fermi energy  $\epsilon_{e,F}$  (or  $\epsilon_{c,F}$ ). For realistic samples of DBRTS, resonant tunneling occurs at a bias  $eV$  much larger than the thermal energy  $k_B T$ . Under this condition, we have  $f_c(\varepsilon) \simeq 0$ . Hence, the *differential* conductance  $G(eV) \equiv (\partial J / \partial V)$  has the simple form

$$G(eV) = \frac{e^2}{\pi\hbar} \int_{-\infty}^{\infty} \sum_{\alpha} T_{\alpha}(\varepsilon) \left( -\frac{\partial f_e(\varepsilon - eV)}{\partial \varepsilon} \right) d\varepsilon. \quad (26)$$

#### IV. SELF-ENERGY AND VERTEX CORRECTION

We will first calculate the lower order self-energy (22) and vertex correction (24), and then generalize the results to the sum over terms of all higher orders.

Let us start with the self-energy. The analytical continuation of the self-energy (22) has been performed by Abrikosov et.al.<sup>30</sup> in details. The key step is to treat  $\varepsilon_1$  as a continuous complex variable and rewrite the summation over  $\varepsilon_1$  into an integral over the path  $C$  as indicated by the solid arrowed curves in Fig. 6a. In this contour integral, the contribution comes from the horizontal path  $\text{Im}[\varepsilon_1] = 0$  and  $\text{Im}[\varepsilon_1] = \varepsilon$ . The resulting self-energy is then analytically continued into the upper half plane of the complex variable  $\varepsilon$ . We then obtain

$$\begin{aligned} \Sigma_R(\alpha, \varepsilon) = & - \left\{ \sum_{\alpha_1, \mathbf{q}} |M_{\alpha\alpha_1}(\mathbf{q})|^2 \int \frac{d\varepsilon_1}{2\pi} \right. \\ & \times \text{Im} \left[ G_R^{(0)}(\alpha_1, \varepsilon_1) \right] D_R^{(0)}(\mathbf{q}, \varepsilon - \varepsilon_1) \tanh \left( \frac{\varepsilon_1}{2k_B T} \right) \left. \right\} \\ & + G_R^{(0)}(\alpha_1, \varepsilon - \varepsilon_1) \text{Im} \left[ D_R^{(0)}(\mathbf{q}, \varepsilon_1) \right] \coth \left( \frac{\varepsilon_1}{2k_B T} \right), \end{aligned} \quad (27)$$

where  $D_R^{(0)}(\mathbf{q}, \varepsilon)$  is a bare phonon Green's function. The contribution from the pole at  $\varepsilon_1 = i\varepsilon$  in Fig. 6a is included in the last term at the right hand side of (27). Using the spectral representation

$$G_R^{(0)}(\alpha, \varepsilon) = \frac{1}{\pi} \left[ \int d\varepsilon_1 \frac{\text{Im} [G_R^{(0)}(\alpha, \varepsilon_1)]}{\varepsilon_1 - \varepsilon - i\delta} \right]_{\delta \rightarrow +0} \quad (28)$$

and a similar form for  $D_R^{(0)}(\mathbf{q}, \varepsilon)$ , we arrive at the final form for the lower order self-energy

$$\begin{aligned} \Sigma_R(\alpha, \varepsilon) = & -\frac{1}{\pi^2} \sum_{\alpha_1, \mathbf{q}} |M_{\alpha\alpha_1}(\mathbf{q})|^2 \int d\omega \int d\varepsilon_1 \\ & \times \frac{\text{Im} [D_R^{(0)}(\mathbf{q}, \omega)] \text{Im} [G_R^{(0)}(\alpha_1, \varepsilon_1)]}{\omega + \varepsilon_1 - \varepsilon - i\delta} \\ & \times [N(\omega) + 1 - f(\varepsilon_1)] , \end{aligned} \quad (29)$$

where  $N(\omega)$  is the Planck distribution function.

To further analyze the above expression, we will adopt a dispersionless bulk LO-phonon spectrum  $\omega_0(\mathbf{q}) \simeq \omega_0$ , which is the commonly used approximation. In this case the phonon Green's functions becomes  $\mathbf{q}$ -independent  $D_R^{(0)}(\mathbf{q}, \omega) \simeq D_R^{(0)}(\omega)$ . Since the system is spatially homogeneous in the  $(x, y)$ -plane, the electronic Green's function does not depend on  $k_{1y}$ , so  $G_R^{(0)}(\alpha_1, \varepsilon_1) = G_R^{(0)}(n_1, \varepsilon_1)$ . Consequently, in (29) the summation over  $(\mathbf{q}, k_{1y})$  acts on the matrix elements  $M_{\alpha\alpha_1}(\mathbf{q})$  alone, and the result derived in Appendix A is

$$\sum_{k_{1y}, \mathbf{q}} |M_{\alpha\alpha_1}(\mathbf{q})|^2 = \frac{M^2}{4\pi^2 l} A_{nn_1} , \quad (30)$$

$$\begin{aligned} A_{nn_1} \equiv & \sqrt{2\pi} \frac{p_2!}{p_1!} \int_0^\infty d\zeta \zeta^{2(p_1-p_2)} e^{-\zeta^2} \\ & \times [L_{p_2}^{p_1-p_2}(\zeta^2)]^2 . \end{aligned} \quad (31)$$

Here  $L_{p_2}^{p_1-p_2}(\zeta^2)$  is the Laguerre polynomial, and  $p_1$  (or  $p_2$ ) is the larger (or smaller) one of  $(n, n_1)$ .

What left to be done in (29) is the two integrations. The integration over  $\omega$  is trivial because of the dispersionless phonon spectrum  $\text{Im}[D_R^{(0)}(\omega)] = -\pi [\delta(\omega - \omega_0) - \delta(\omega + \omega_0)]$ . Since in realistic DBRTS samples the  $\gamma$  is less than 0.5 meV which is much less than the

thermal energy  $k_B T$  in the problem of our interest here, the integration over  $\varepsilon_1$  can be carried out with the residual method. Together with the equality  $N(-\omega) = -1 - N(\omega)$ , we obtain the simple form

$$\begin{aligned}\Sigma_R(\alpha, \varepsilon) = & \frac{M^2}{4\pi^2 l} \sum_{n_1} A_{nn_1} \left[ \frac{N(\hbar\omega_0) + f(E_{n_1})}{\varepsilon - E_{n_1} + \hbar\omega_0 + i\gamma/2} \right. \\ & \left. + \frac{N(\hbar\omega_0) + 1 - f(E_{n_1})}{\varepsilon - E_{n_1} - \hbar\omega_0 + i\gamma/2} \right].\end{aligned}\quad (32)$$

The important quantity is the imaginary part

$$\begin{aligned}\text{Im} [\Sigma_R(\alpha, \varepsilon)] = & -\frac{M^2}{4\pi^2 l} \sum_{n_1} A_{nn_1} \\ & \frac{\gamma}{2} \left[ \frac{N(\hbar\omega_0) + f(E_{n_1})}{(\varepsilon - E_{n_1} + \hbar\omega_0)^2 + (\gamma^2/4)} \right. \\ & \left. + \frac{N(\hbar\omega_0) + 1 - f(E_{n_1})}{(\varepsilon - E_{n_1} - \hbar\omega_0)^2 + (\gamma^2/4)} \right]\end{aligned}\quad (33)$$

which will be discussed later.

Now we come to the vertex correction  $\mathcal{K}(\alpha, \varepsilon)$  in (24). The procedure of analytical continuation is similar to that for the self-energy  $\Sigma_R(\alpha, \varepsilon)$ , but using the contour of integration in Fig. 6b. After all algebraic manipulations, we obtain

$$\begin{aligned}\mathcal{K}(\alpha, \varepsilon) = & 2\pi \sum_{\alpha_1, \mathbf{q}} |M_{\alpha\alpha_1}(\mathbf{q})|^2 \int \frac{d\varepsilon_1}{2\pi} \left[ \mathcal{P} \tanh \left( \frac{\varepsilon_1}{2k_B T} \right) \right. \\ & \left. + \mathcal{Q} \coth \left( \frac{\varepsilon_1}{2k_B T} \right) \right],\end{aligned}\quad (34)$$

where

$$\begin{aligned}\mathcal{P} \equiv & D_A^{(0)}(\varepsilon - \varepsilon_1 - \Omega) G_R^{(0)}(n_1, \varepsilon_1 + \Omega) \text{Im}[G_R^{(0)}(n_1, \varepsilon_1)] \\ & + D_R^{(0)}(\varepsilon - \varepsilon_1 - \Omega) G_A^{(0)}(n_1, \varepsilon_1) \text{Im}[G_R^{(0)}(n_1, \varepsilon_1 + \Omega)] \\ \mathcal{Q} \equiv & \text{Im}[D_R^{(0)}(\varepsilon_1)] \\ & \times G_R^{(0)}(n_1, \varepsilon - \varepsilon_1) G_A^{(0)}(n_1, \varepsilon - \varepsilon_1 - \Omega).\end{aligned}\quad (35)$$

At this stage, one can set  $\Omega \rightarrow 0$ . Following the same argument which leads (29) to (32), the vertex correction is derived as

$$\begin{aligned}\mathcal{K}(\alpha, \varepsilon) = & \frac{M^2}{2\pi l} \sum_{n_1} A_{nn_1} \left[ \frac{N(\hbar\omega_0) + f(\varepsilon + \hbar\omega_0)}{(\varepsilon - E_{n_1} + \hbar\omega_0)^2 + (\gamma^2/4)} \right. \\ & \left. + \frac{N(\hbar\omega_0) + 1 - f(\varepsilon - \hbar\omega_0)}{(\varepsilon - E_{n_1} - \hbar\omega_0)^2 + (\gamma^2/4)} \right].\end{aligned}\quad (36)$$

Comparing this expression with (33), we see that at the lowest order of electron-phonon interaction, the self-energy and the vertex correction have similar structure. In particular, for the situation very close to resonance  $\varepsilon \pm \omega_0 \approx E_{n_1}$ , which is the main interest of the present work, we establish the following relation

$$\mathcal{K}(\alpha, \varepsilon) = \frac{4\pi |\text{Im} [\Sigma_R(\alpha, \varepsilon)]|}{\gamma} \quad (37)$$

between the self-energy and the vertex correction. It is important to point out that the above relation (37) holds up to any order of electron-phonon coupling, provided that the phonon spectrum is assumed dispersionless<sup>31,27,28</sup>. Consequently, from now on we only need to analyze the single electron self-energy.

All above results were derived with the only approximation that the weak dispersion of the LO phonon spectrum can be ignored. If the tunneling is not resonant, these results are accurate enough to be compared with experiments at all temperatures. They are also reliable if at low temperature the thermal energy is much smaller than the LO phonon energy. However, since we are interested in resonant magnetotunneling at finite temperatures, higher order electron-phonon interaction must be included in the self-energy and the vertex correction. This problem is exactly solvable if only two Landau levels  $n = 0$  and  $n = 1$  in the well dominate the tunneling process. As described at the end of Sec. II for our model, this two-level system can be realized by fixing the concentration of impurities in the emitter. For the phonon absorption resonant magnetotunneling process, the tunneling electrons are emitted from the Landau level  $n_e = 0$  in the emitter. On the other hand, for the phonon emission resonant magnetotunneling process, the emitting Landau level is  $n_e = 1$ . From now on we will restrict ourselves to such two-level system.

The procedure of calculating the contribution to self-energy by any order of electron-phonon interaction is the same as that by the lowest order. Analysis of analytical con-

tinuation leads to the following rule of constructing diagrams. We introduce two kinds of phonon lines: a dotted line describes a absorption process with a Bose factor  $N(\hbar\omega_0)$ , while a dashed one corresponds to a phonon emission with a factor  $N(\hbar\omega_0) + 1$ . Then, each dotted line should be followed by a dashed line, and vice versa. Consequently, all even order contributions vanish, and only the diagrams with odd number of phonon lines survive. As an example, the third order diagram is shown in Fig. 7. Based on the diagrammatic analysis, the  $\nu$ th order contribution contains  $2\nu$  electron-phonon vertices,  $\nu$  factors  $g^2 A_{01}$  with  $g^2(B) \equiv M^2/4\pi^2l$ ,  $\nu$  phonon factors  $N(\omega_0) + 1/2 \mp 1/2$ , and  $2\nu - 1$  electron Green's functions. Therefore, the final form of each order's contribution is very similar to (32), except that there is only one term in the summation of  $n_1$ , and  $A_{01} \simeq 1$ .

We will not present here the detailed calculation, but will only show the final results. Since our model neglects the electron-electron interaction in the well, it is equivalent to the case that in the well the occupation probability of each electronic eigenstate is negligible. Then, including all orders in  $g$ , the electron self-energy is obtained as

$$\begin{aligned} \Sigma_R(\alpha, \varepsilon) = & \sum_{s=0}^{\infty} \left[ \frac{g^{2(2s+1)} N^{s+1} (N+1)^s}{(\varepsilon - E_{n_1} + \hbar\omega_0 + i\gamma/2)^{2s+1} (\varepsilon - E_n + i\gamma/2)^{2s}} \right. \\ & \left. + \frac{g^{2(2s+1)} N^s (N+1)^{s+1}}{(\varepsilon - E_{n_1} - \hbar\omega_0 + i\gamma/2)^{2s+1} (\varepsilon - E_n + i\gamma/2)^{2s}} \right] \end{aligned} \quad (38)$$

where  $N \equiv N(\hbar\omega_0)$  is the Planck function. When  $\varepsilon \simeq E_0$  and so  $E_{n_1} = E_1$ , the first term in (38) gives the phonon absorption resonant magnetotunneling. On the other hand, when  $\varepsilon \simeq E_1$  and so  $E_{n_1} = E_0$ , the phonon emission resonant magnetotunneling is represented by the second term in (38).

## V. SELF-CONSISTENT RENORMALIZATION

Studies on resonance effects at very low temperatures in both free electron gas<sup>27,28</sup> and in DBRTS<sup>20,22</sup> indicate that resonant states are strongly coupled, and the perturbation expansion should be renormalized. A so-called self-consistent renormalization can be used, which

replaces all bare electron Green's functions in the self-energy formula with the corresponding dressed ones, resulting in self-energy equations.

Let us first renormalize the first order self-energy to review the phonon emission process in which the tunneling electron starts from the Landau level  $n_e = 1$  in the emitter. The self-consistent equation is simply

$$\Sigma_R(\alpha, \varepsilon) = \frac{g^2}{\varepsilon - E_0 - \hbar\omega_0 + \Sigma_R(\alpha, \varepsilon) + i\gamma/2}. \quad (39)$$

Very near to the resonant  $\varepsilon - E_0 - \hbar\omega_0 = 0$  and  $\hbar\omega_0 = \hbar\omega_c$ , this self-consistent equation has the solution

$$\Sigma_R(\alpha, \varepsilon) \simeq (E_0 + \hbar\omega_0 - \varepsilon)/2 \pm g, \quad (40)$$

which will produce the Landau levels anti-crossing phenomenon<sup>20,22</sup>. For a 2D free electron gas. the higher-order corrections has been analyzed in Ref. 32.

Now let us turn to the main theme of the present work: finite temperature phonon assisted resonant magnetotunneling. Here both phonon emission and phonon absorption are involved, and we must use (38) as the basis for the renormalization. If we define  $\Sigma_R(n, \varepsilon) \equiv \Sigma_R(\alpha, \varepsilon)$  and  $G_R(n, \varepsilon) \equiv G_R(\alpha, \varepsilon)$  for  $\alpha = (n, k_y)$ , then the self-consistent equation can be expressed as

$$\begin{aligned} \Sigma_R(1, \varepsilon + \hbar\omega_0) &= \sum_{s=0}^{\infty} g^{2(2s+1)} N^s(\hbar\omega_0) [N(\hbar\omega_0) + 1]^{s+1} G_R^{2s+1}(0, \varepsilon) G_R^{2s}(1, \varepsilon + \hbar\omega_0), \\ \Sigma_R(0, \varepsilon) &= \sum_{s=0}^{\infty} g^{2(2s+1)} N^{s+1}(\hbar\omega_0) [N(\hbar\omega_0) + 1]^s G_R^{2s}(0, \varepsilon) G_R^{2s+1}(1, \varepsilon + \hbar\omega_0). \end{aligned} \quad (41)$$

Let us define the temperature dependent coupling constant  $\mu \equiv g^2 \sqrt{N(\hbar\omega_0)[N(\hbar\omega_0) + 1]}$ , the dimensionless thermal factor  $\nu \equiv \sqrt{N(\hbar\omega_0)/[N(\hbar\omega_0) + 1]}$ , and

$$L(\varepsilon) \equiv \frac{\mu G_R(0, \varepsilon) G_R(1, \varepsilon + \hbar\omega_0)}{1 - \mu^2 [G_R(0, \varepsilon) G_R(1, \varepsilon + \hbar\omega_0)]^2}. \quad (42)$$

If we further define

$$\theta(\varepsilon) \equiv \frac{\varepsilon - (E_0 + E_1 - \hbar\omega_0 - i\gamma)/2}{\sqrt{\mu}},$$

$$\delta \equiv \frac{|E_0 - E_1 + \hbar\omega_0|}{2\sqrt{\mu}},$$

then, we can rewrite (41) as

$$\begin{aligned}\Sigma_R(1, \varepsilon + \hbar\omega_0) &= \sqrt{\mu}[\theta(\varepsilon) + \delta] \frac{L(\varepsilon)/\nu}{1 + L(\varepsilon)/\nu} \\ \Sigma_R(0, \varepsilon) &= \sqrt{\mu}[\theta(\varepsilon) - \delta] \frac{\nu L(\varepsilon)}{1 + \nu L(\varepsilon)} \\ G_R(1, \varepsilon + \hbar\omega_0) &= \frac{1}{\sqrt{\mu}} \frac{1 + L(\varepsilon)/\nu}{\theta(\varepsilon) + \delta} \\ G_R(0, \varepsilon) &= \frac{1}{\sqrt{\mu}} \frac{1 + \nu L(\varepsilon)}{\theta(\varepsilon) - \delta}.\end{aligned}\tag{43}$$

Substituting the last two equations of (43) into (42), we obtain the equation

$$\frac{[1 \pm \sqrt{1 + 4L^2}][1 + L(\nu + 1/\nu) + L^2]}{2L} = \theta^2(\varepsilon) - \delta^2\tag{44}$$

to solve for  $L(\varepsilon)$ . Knowing  $L(\varepsilon)$ , we go back to the first two equations of (43) to calculate the renormalized self-energies  $\Sigma_R(1, \varepsilon + \hbar\omega_0)$  and  $\Sigma_R(0, \varepsilon)$ .

## VI. RESULTS

We will solve (44) for a temperature corresponding to  $\gamma \ll \sqrt{\mu}$ . There are several branches of solutions, and the proper one should be chosen according to the correct analytical properties and asymptotic behavior of the Green's functions. In general, the asymptotics of Green's functions at large  $\varepsilon$  is  $1/\varepsilon$ . Consequently, the correct branch of solutions should correspond to  $\lim_{\varepsilon \rightarrow \infty} L(\varepsilon) = 0$ .

Let us first check a limiting resonant tunneling case. At  $|\theta(\varepsilon)|^2 - \delta^2 \ll 1$ , the proper solution corresponds to  $|1 + L(\varepsilon)/\nu| \ll 1$ . Therefore, we obtain  $L(\varepsilon) \simeq -\nu$ , which yield the solutions  $G_R(1, \varepsilon) \rightarrow 0$  and  $G_R(0, \varepsilon) \rightarrow \sqrt{\mu}(1 - \nu^2)/[\theta(\varepsilon) - \delta]$ . We see that in the phonon absorption process, the original elastic resonant tunneling peak in the transparency spectrum survives, and its position is not affected by the electron-phonon scattering. This is in contrast to the phonon emission process, where the original elastic resonant tunneling

peak splits symmetrically into a doublet of almost equal strength. At sufficiently high temperature  $k_B T \gg \hbar\omega_0$ ,  $\nu \rightarrow 1$  and then both  $G_R(0, \varepsilon)$  and  $G_R(0, \varepsilon)$  approach zero.

This solution of limiting case will be used as the initial input when solving the self-consistent equation (44) numerically. We will study the case that one electron tunnels into the well from the  $n_e = 0$  Landau level in the emitter, under the exact resonant condition  $\delta = 0$ . We also choose  $\gamma = 0.11g$ . Two temperatures are used in our calculation:  $T=174$  K (corresponding to  $\nu=0,3$ ) with  $\text{Im}[\theta(\varepsilon)]=0.1$ , and  $T=74$  K (corresponding to  $\nu=0,006$ ) with  $\text{Im}[\theta(\varepsilon)]=0.23$ . For a given value of  $\text{Re}[\theta(\varepsilon)]$ , we solve (44) for both  $\text{Re}[L(\varepsilon)]$  and  $\text{Im}[L(\varepsilon)]$ , and then plot them in Fig. 8. The dotted contour is for  $T=174$  K with  $\text{Re}[\theta(\varepsilon)]$  varies along the contour from -4 to -0.2, and then from 0.2 to 4. For the other temperature  $T=74$  K, the solution is the crossed curve with  $\text{Re}[\theta(\varepsilon)]$  varies from -5 to -0.4, and then from 0.4 to 5.

Based on the solution in Fig. 8, the corresponding dimensionless transmission probability  $K_0(\varepsilon)g^2$  [defined by (15) and (16)] is calculated, and the results are shown in Fig. 9a as functions of reduced energy  $\text{Re}[\theta(\varepsilon)]\sqrt{\mu}/g$ . In the absence of electron-phonon scattering, the sharp peak of transmission probability is marked as the curve 1. When the electron-phonon interaction is turned on, two inelastic wings are formed with increasing strength as the temperature is raised from  $T=74$  K (curve 2) to  $T=174$  K (curve 3). In order to demonstrate these inelastic wings more clearly, we use (17) to decompose the transmission peak  $K_0(\varepsilon)$  into the main peak  $K_0^0(\varepsilon)$  and the inelastic wings  $K_0^v(\varepsilon)$ . The results are plotted in Fig. 9b where curve 1) shows the main peak (for both temperatures), and where curve 2) and curve 3) show respectively the inelastic wings for  $T = 74K$  and  $T = 174K$ . For both temperatures, within the accuracy of our plotting, the broadening of  $K_0^0(\varepsilon)$  due to the virtual phonon processes can not be detected because it can not be distinguished from the pure elastic peak. On the other hand, the temperature dependence of the inelastic wings is quite dramatic.

The phonon absorption process is entirely different from the phonon emission process, which we have also calculated here and found the separation between the two resolved sharp peaks being proportional to  $2g$ . The physical origin of this difference is that the phonon

emission is a coherent process for which the electron-phonon system remains coherent, while the phonon absorption is typically an incoherent process since absorbed real phonons have random phases.

## VII. REMARKS

As demonstrated in the previous section, the absorption of real phonons during the resonant tunneling yields only minor corrections in the elastic main peak of the transparency spectrum. On the other hand, the inelastic process indeed produces two broad wings in the spectrum, the strength of which is sensitive to the resonant condition and grows with increasing temperature. If the tunneling current and so the differential conductance  $G(eV)$  can be measured in this way, we can further extract informations of the dynamical tunneling process as follows. Since the tunneling is dominated by the transmission probability of only one channel,  $T_0(\varepsilon)$ , (26) can be inverted to the form

$$T_0(\varepsilon) = \frac{2\hbar}{e^2 k_B T} \int_0^\infty d\xi \int_{-\infty}^\infty d\mu \times \cos\left(\frac{\varepsilon - \epsilon_{e,F} - \mu}{k_B T} \xi\right) \frac{\sinh \xi}{\xi} G(\mu). \quad (45)$$

Substituting the measured  $G(eV)$  into the integrand and performing a numerical integration, the transparency spectrum  $T_0(\varepsilon)$  can then be *measured*.

The self-energy (33) has a similar form as that obtained by Fertig et.al.<sup>26</sup> for a resonant tunneling system interacting with impurities under an applied magnetic field. While in both cases the magnetic field broadens the width of the resonant tunneling peak because of the violation of selection rules for the parallel momentum, there are two important differences. In our case the broadening reaches its maximum value when  $\varepsilon = E_{n_1} \pm \hbar\omega_0$ . Furthermore, the self-energy due to the electron-phonon interaction is proportional to  $B^{1/2}$ , but for the electron-impurity scattering it is proportional to  $B$ .

The present work is partially supported by the Norwegian Research Council, Grant No. 100267/410.

## APPENDIX A: SUMMATION OF ELECTRON-LO PHONON MATRIX ELEMENTS

We will calculate the  $(k_{1y}, \mathbf{q})$  summation of the electron-LO phonon matrix elements

$$\begin{aligned} \sum_{k_{1y}, \mathbf{q}} |M_{\alpha\alpha_1}(\mathbf{q})|^2 &= \sum_{k_{1y}, \mathbf{q}} \frac{M^2}{V_0 q^2} \int dx dy dz dx' dy' dz' \\ &\times e^{-\mathbf{q}\mathbf{r}} e^{\mathbf{q}\mathbf{r}'} \phi_{\alpha_1}^*(\mathbf{r}) \phi_\alpha(\mathbf{r}) \phi_\alpha^*(\mathbf{r}') \phi_{\alpha_1}(\mathbf{r}'). \end{aligned} \quad (\text{A1})$$

First, we transform the summation into integrations. Since the Green's functions are independent of  $k_y$ , we can conveniently choose  $k_y = 0$ . Therefore, we have

$$\begin{aligned} \sum_{k_{1y}, \mathbf{q}} |M_{\alpha\alpha_1}(\mathbf{q})|^2 &= \int \frac{V_0 d^3 \mathbf{q}}{(2\pi)^3} \int \frac{l dk_{y1}}{2\pi} |M_{\alpha\alpha_1}(\mathbf{q})|^2 \\ &= \int \frac{d^3 \mathbf{q}}{(2\pi)^3} \frac{M^2 l}{q^2} \int dx dx' dz dz' \\ &\times \chi^*(z) \chi(z) \chi^*(z') \chi(z') e^{ilq_x(x-x')} e^{idq_z(z-z')} \\ &\times \varphi_{n_1}^*(x - l^2 q_y) \varphi_{n_1}(x' - l^2 q_y) \varphi_n^*(x') \varphi_n(x). \end{aligned} \quad (\text{A2})$$

The  $\mathbf{q}$  integration can now be performed to give

$$\begin{aligned} &\int \frac{dq_x dq_z \exp [iq_x(x-x') + iq_z(z-z')]}{(2\pi)^2} \\ &= \frac{1}{2\pi} K_0 \left[ |q_y| \sqrt{(z-z')^2 + (x-x')^2} \right], \end{aligned} \quad (\text{A3})$$

where  $K_0$  is the McDonald function.

For realistic DBRTS samples, the width  $d$  of the quantum well is much smaller than the magnetic length  $l$ . In this case the difference  $z-z'$  in the argument of the McDonald function can be ignored, and the integration over  $z$  and  $z'$  is equal to 1 because of the normalization condition. By introducing two new dimensionless variables  $\xi \equiv q_y l$ ,  $\eta \equiv (x - x')/l$ , and  $\zeta \equiv x/l$  we arrive at the final expression

$$\sum_{k_{1y}, \mathbf{q}} |M_{\alpha\alpha_1}(\mathbf{q})|^2 = \frac{M^2}{(2\pi)^2 l} A_{nn_1}, \quad (\text{A4})$$

where

$$\begin{aligned}
A_{nn_1} \equiv & \int d\zeta d\xi d\eta K_0(|\eta\xi|) \\
& \times \tilde{\varphi}_{n_1}^* \left( \zeta - \frac{\xi - \eta}{2} \right) \tilde{\varphi}_{n_1} \left( \zeta - \frac{\xi + \eta}{2} \right) \\
& \times \tilde{\varphi}_n^* \left( \zeta + \frac{\eta - \xi}{2} \right) \tilde{\varphi}_n \left( \zeta + \frac{\eta + \xi}{2} \right). \tag{A5}
\end{aligned}$$

Substituting the harmonic oscillator wave functions

$$\tilde{\varphi}_n(\zeta) = \left( \frac{1}{\sqrt{\pi} 2^n n!} \right)^{1/2} e^{-\zeta^2/2} H_n(\zeta) \tag{A6}$$

into the above integrand, where  $H_n(\zeta)$  is the Hermite polynomial, we obtain the results given by (31).

## REFERENCES

<sup>1</sup> R. Tsu and L. Esaki, *Appl. Phys. Lett.* **22**, 562 (1973).

<sup>2</sup> T. C. L. G. Sollner, W. D. Goodhue, P. E. Tannenwald, C. D. Parker, and D. D. Peck, *Appl. Phys. Lett.* **43**, 588 (1983).

<sup>3</sup> B. Ricco and M. Ya. Azbel, *Phys. Rev. B* **29**, 1970 (1984).

<sup>4</sup> P. J. Price, *Phys. Rev. B* **38**, 1994 (1988); M. Büttiker, *IBM J. Res. Dev.* **32**, 63 (1988); A. R. Bonnefoi, T. C. McGill, and R. D. Buhrman, *Phys. Rev. B* **37**, 8754 (1988); G. Kim and G. B. Arnold, *Phys. Rev. B* **38**, 3252 (1988).

<sup>5</sup> S. Luryi, *Appl. Phys. Lett.* **47**, 490 (1985).

<sup>6</sup> T. Weil and B. Winter, *Appl. Phys. Lett.* **50**, 1281 (1987); M. Jonson and Anna Grincwaig, *Appl. Phys. Lett.* **51**, 1729 (1987).

<sup>7</sup> W. R. Frensley, *Phys. Rev. Lett.* **57**, 2853 (1986); *Phys. Rev. B* **36**, 1570 (1987).

<sup>8</sup> V. J. Goldman, D. C. Tsui, and J. Cunningham, *Phys. Rev. B* **36**, 7635 (1987).

<sup>9</sup> L. I. Glazman, R. I. Shekhter, *Sov. Phys. JETP* **67**, 163 (1988).

<sup>10</sup> N. S. Wingreen, K. W. Jacobsen, and J. W. Wilkins, *Phys. Rev. Lett.* **61**, 1396 (1988).

<sup>11</sup> Ned S. Wingreen, Karsten W. Jacobsen, and John W. Wilkins, *Phys. Rev. B* **40**, 11834 (1989).

<sup>12</sup> W. Cai, T. F. Zheng, P. Hu, B. Yudanin, and M. Lax, *Phys. Rev. Lett.* **63**, 418 (1989).

<sup>13</sup> D. Sokolovski, *Phys. Rev. B* **37**, 4201 (1988).

<sup>14</sup> M. Jonson, *Phys. Rev. B* **39**, 5924 (1989).

<sup>15</sup> P. Johansson, *Phys. Rev. B* **41**, 9892 (1990).

<sup>16</sup> E. E. Mendez, L. Esaki, and W. I. Wang, *Phys. Rev. B* **33**, 2893 (1986).

<sup>17</sup> M. L. Leadbeater, E. S. Alves, L. Eaves, M. Henini, O. H. Hughes, A. Celeste, J. C. Portal, G. Hill, and M. A. Pate, Phys. Rev. B **39**, 3438 (1989).

<sup>18</sup> C. H. Yang, M. J. Yang, and Y. C. Kao, Phys. Rev. B **40**, 6272 (1989).

<sup>19</sup> S. Das Sarma, Phys. Rev. Lett. **52**, 859 (1984); **52**, 1570(E) (1984); D. M. Larsen, Phys. Rev. B **30**, 4807 (1984); F. M. Peeters and J. T. Devreese, Phys. Rev. B **31**, 3689 (1985).

<sup>20</sup> G. S. Boebinger, A. F. S. Levi, S. Schmitt-Rink, A. Passner, L. N. Preiffer, and K. W. West, Phys. Rev. Lett. **65**, 235 (1990).

<sup>21</sup> J. G. Chen, C. Y. Yang, M. J. Yang, and R. A. Wilson, Phys. Rev. B **43**, 4531 (1991).

<sup>22</sup> Nanzhi Zou, K. A. Chao, and Yu. M. Galperin, Phys. Rev. Lett. **71**, 1756 (1993).

<sup>23</sup> G. D. Mahan, *Many Particle Physics* (Plenum, New York, 1981).

<sup>24</sup> Nanzhi Zou, J. Rammer, and K. A. Chao, Phys. Rev. B **46**, 15912 (1992).

<sup>25</sup> J. Bardeen, Phys. Rev. Lett. **6**, 57 (1961).

<sup>26</sup> H. A. Fertig, Song He, and S. Das Sarma, Phys. Rev. B **41**, 3596 (1990)

<sup>27</sup> Y. B. Levinson, and E. I. Rashba, Usp. Fiz. Nauk, **11**(4), 683 (1973).

<sup>28</sup> Y. B. Levinson, and E. I. Rashba, Rep. Prog. Phys., **36**, 1499 (1973).

<sup>29</sup> I. B. Levinson, A. Yu. Matulis, and L. M. Shcherbakov, Sov. Phys. JETP **33**, 464 (1971) [Zh. Eksp. Teor. Fiz. **60**, 859 (1971)].

<sup>30</sup> A. A. Abrikosov, L. P. Gorkov, and I. E. Dzyaloshinski, *Methods of Quantum Field Theory in Statistical Physics* (Dover Publications, inc., New York, 1975).

<sup>31</sup> Yu. A. Firsov, V. L. Gurevich, R. V. Parfeniev, I. M. Tsidilkovskii, *Landau Level Spectroscopy*, ed. by G. Landwehr and E.I. Rashba, Elsevier Science Publishers B.V. (1991), p.1183.

<sup>32</sup> I. B. Levinson, A. Yu. Matulis, and L. M. Shcherbakov, Sov. Phys. JETP **33**, 594 (1971) [Zh. Eksp. Teor. Fiz. **60**, 1097 (1971)].

## FIGURES

FIG. 1. A schematic illustration of a double-barrier resonant tunneling structure (DBRTS).

FIG. 2. Diagrams illustrate phonon-assisted resonant magnetotunneling as the magnetic field is tuned into the resonant condition where the Landau level separation  $\hbar\omega_c$  equals the optical phonon energy  $\hbar\omega_0$ : A) A phonon *emission* process leading to two coherent final states ( $E_0$  and  $E_1$ ), and b) a phonon *absorption* process leading to two final states ( $A_0$  and  $A_1$ ).

FIG. 3. Diagrammatic representation for the two-particle transmission Green's function  $K_{\alpha\alpha_1}(\varepsilon, \varepsilon_1)$ .

FIG. 4. Diagrammatic representation for the total transmission  $K_\alpha(\varepsilon)$  given by Eqs. (17)-(19).

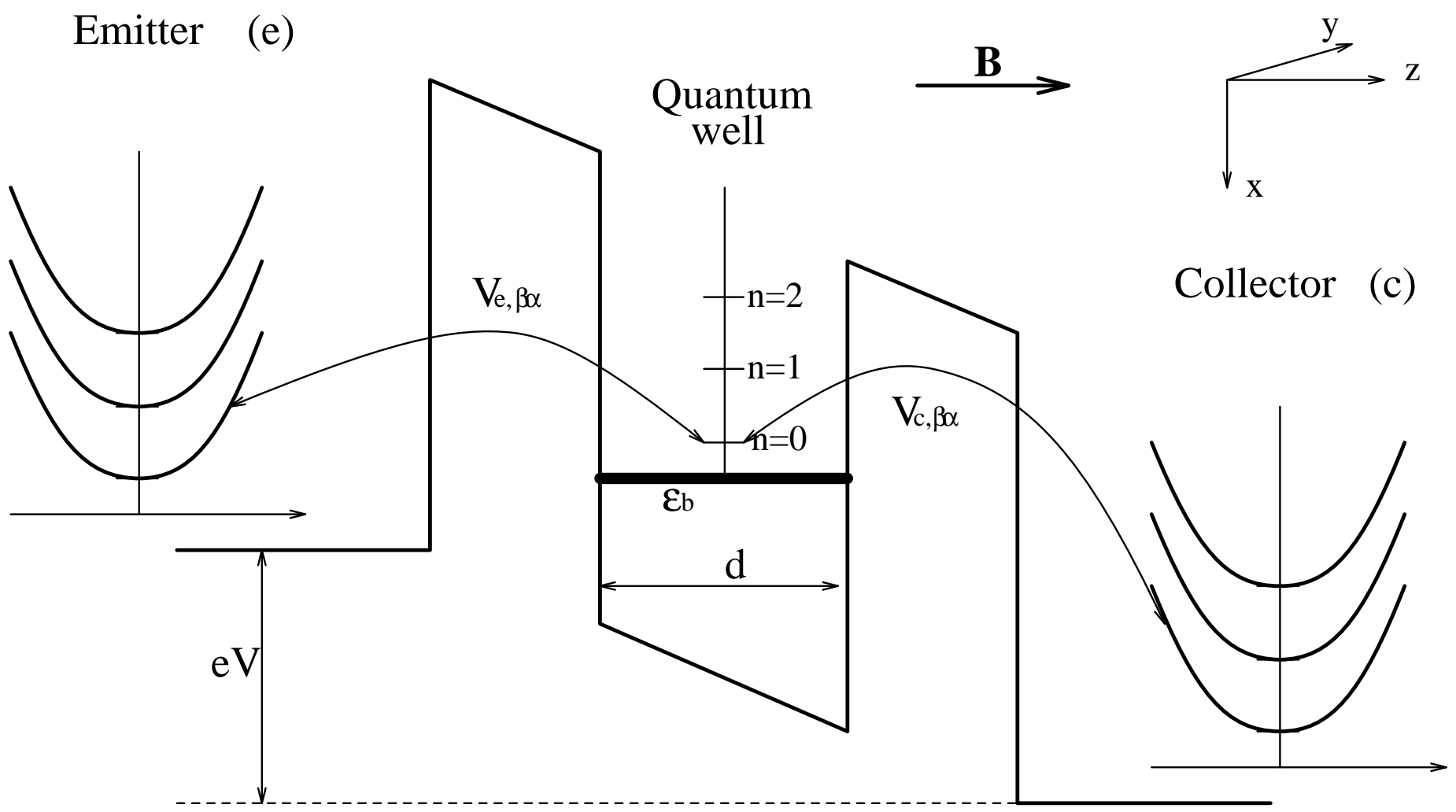
FIG. 5. Lowest order diagrams for (a) the self-energy  $\Sigma(\alpha, \varepsilon)$ , and (b) the vertex Green's function  $\mathcal{K}(\alpha, \varepsilon)$ .

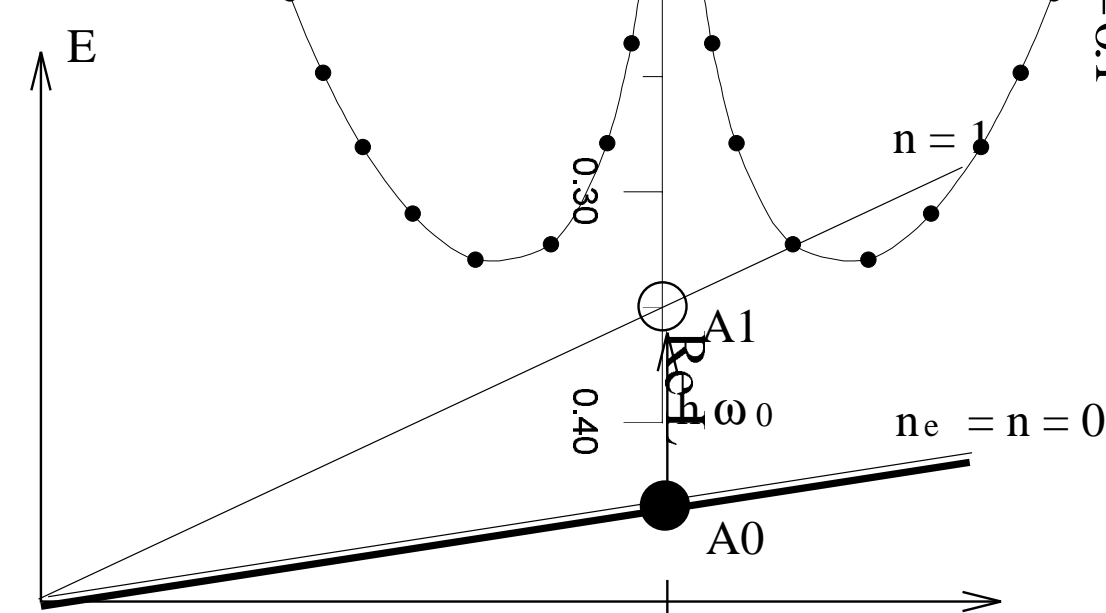
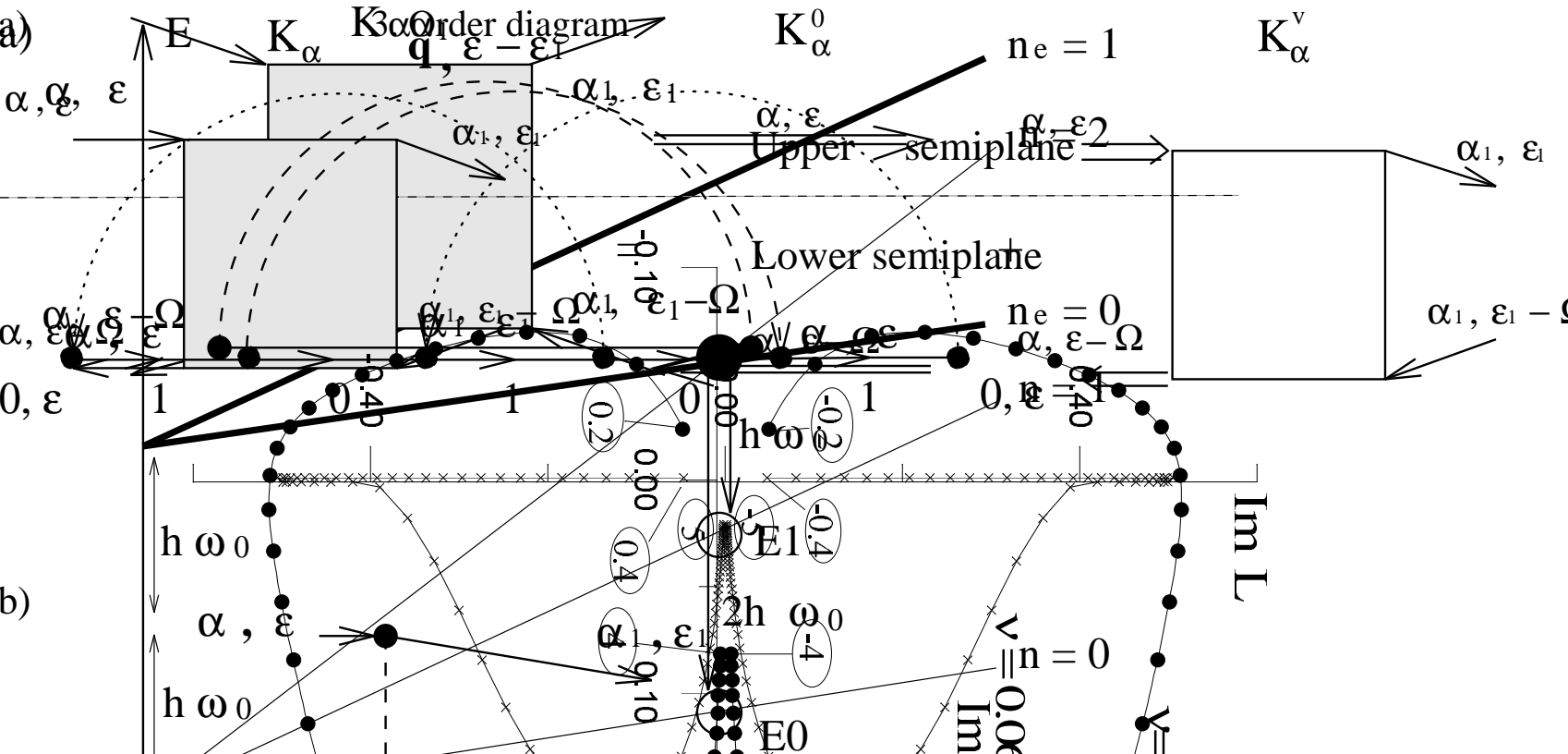
FIG. 6. Contours of integration for (a) the self-energy  $\Sigma(\alpha, \varepsilon)$ , and (b) the vertex Green's function  $\mathcal{K}(\alpha, \varepsilon)$ .

FIG. 7. Resonant third order diagram for the self-energy. A dotted line denotes a phonon absorption process, while a dashed line denotes an emission process. The electron lines are marked by their Landau level numbers.

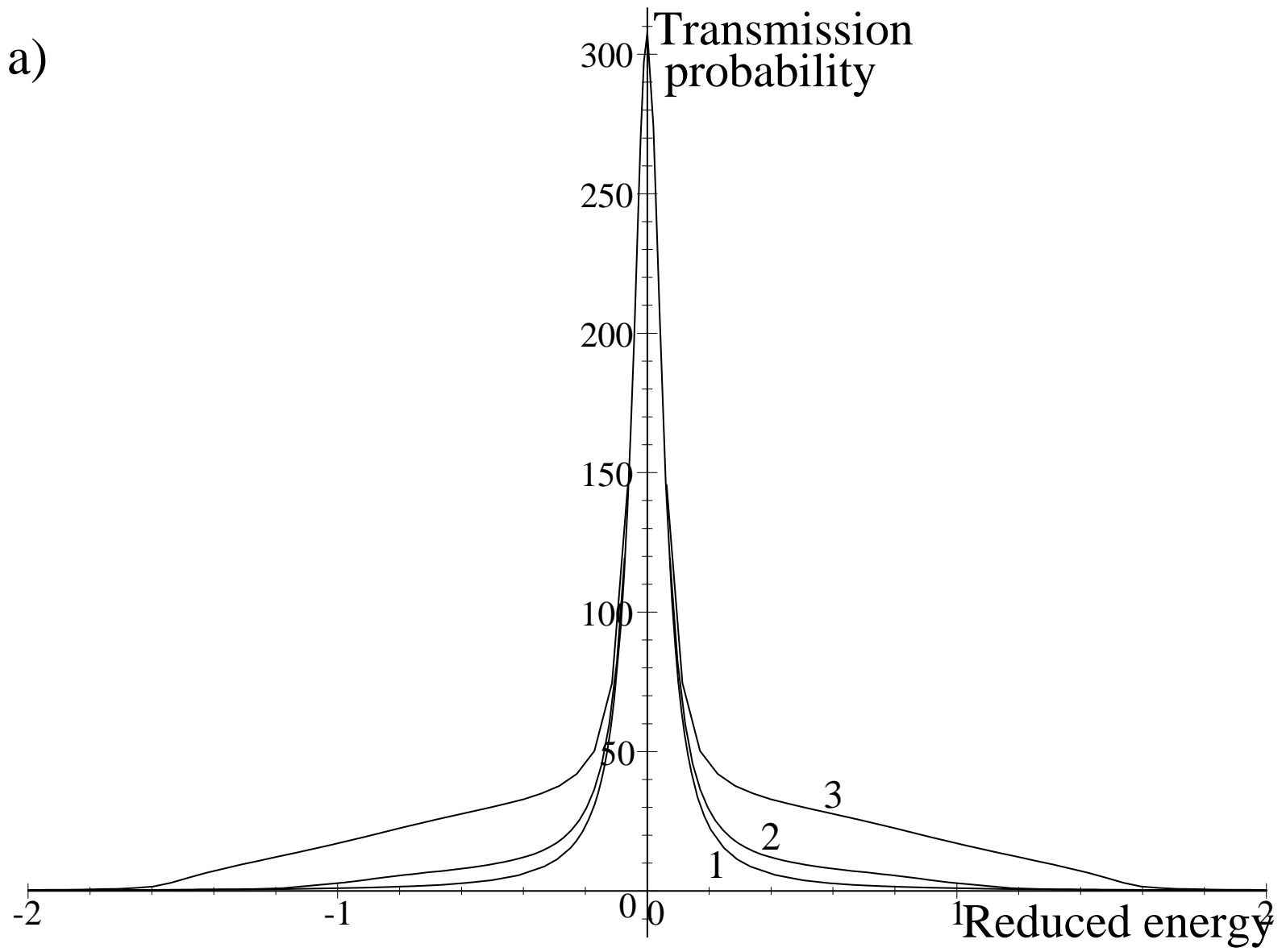
FIG. 8. Solution  $\text{Re}[L(\omega)]$  and  $\text{Im}[L(\omega)]$  of Eq. (44) for  $\delta = 0$  and  $\gamma = 0.11g$ . Dotted contour is for temperature  $T=174$  K, and crossed contour is for  $T=74$  K.

FIG. 9. Phonon absorption resonant magnetotunneling spectrum corresponding to the solution in Fig. 8. A) The dimensionless transmission probability  $K_0(\varepsilon)g^2$  is plotted as function of the reduced energy  $\text{Re}[\theta(\varepsilon)]\sqrt{\mu}/g$ . Curve 1) shows the transmission probability in the absence of electron-phonon scattering, while curve 2) and curve 3) show respectively the results at  $T = 74K$  and at  $T = 174K$ . B) Transmission spectrum decomposed into main peak  $K_0^0(\varepsilon)g^2$  (curve 1) and inelastic wings  $K_0^\nu(\varepsilon)g^2$  at  $T = 74K$  (curve 2) and  $T = 174K$  (curve 3).





a)



b)

